Inorganic Chemistry

Article

pubs.acs.org/IC

Interaction of Various Gas Molecules with Paddle-Wheel-Type Open Metal Sites of Porous Coordination Polymers: Theoretical Investigation

Yuh Hijikata and Shigeyoshi Sakaki*

Fukui Institute for Fundamental Chemistry, Kyoto University, Takano-Nishihiraki-cho 34-4, Sakyo-ku, Kyoto 606-8103, Japan

Supporting Information

ABSTRACT: We theoretically evaluated binding energies (E_b's) between various gas molecules and the Cu center open metal site (Cu-OMS) of Cu paddle-wheel units, $[Cu_2(O_2CR)_4]$ (R = H, Me, or Ph) using density functional theory (DFT) and MP2−MP4. The optimized geometry of the model system $[Cu_2(O_2CPh)_4]$ agrees with the experimental structure. The E_b of CO with $[Cu_2(O_2CH)_4]$ is only slightly different between the open-shell singlet and triplet states. The calculated E_b decreases in the order MeNC > H_2O > MeCN > C_2H_4 > C_2H_2 > CO > CO_2 > N_2 > CH_4 > H_2. The trend is discussed in terms of the electrostatic interaction energy (ES), exchange repulsion energy (EX), and charge-transfer (CT) + polarization (Pol) interaction energy at the Hartree−Fock level and the electron correlation effect. The ES increases linearly with an increase in E_b, while the EX decreases linearly with an increase in E_b. These relationships indicate that the ES compensates for the EX. In other words, the E_b does not depend on the sum of ES and EX, which corresponds to the static energy. The electron correlation effect contributes little to the above-mentioned decreasing order of E_b. The total E_b roughly increases with an increase in the CT+Pol term, suggesting that the CT+Pol term plays important roles in determining the trend of E_b. The shift of the stretching frequency of adsorbed gas molecules on the Cu-OMS is reproduced well by the DFT calculation with the model system $[Cu_2(O_2CH)_4(L)_2]$ (L = gas molecule). We found that the positive charge on the Cu significantly contributes to the shift in the end-on coordination gas molecules such as CO, MeNC, MeCN, and N_2. Although the shift has been generally discussed in terms of donation and back-donation, the present result indicates that the electrostatic potential field in the porous coordination polymer should be considered in the discussion of the frequency shift.

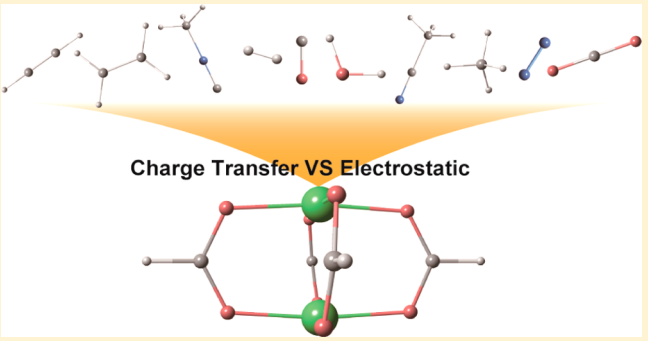

INTRODUCTION

Recently, porous coordination polymers (PCPs) or metal−organic frameworks (MOFs),[1,2] which consist of metal ions and organic ligands, have attracted a lot of interest as novel porous materials. This is because they have great potential for gas storage as a result of high surface areas[3−5] and gas separation because of their various pore shapes, structural flexibilities, and various affinity sites,[6−9] as well as possibilities of catalysis by organic ligands and/or metal sites.[10,11] The host−guest interaction plays a crucial role in producing these functions of PCPs. Metal ions in frameworks sometimes form coordinatively unsaturated sites known as open metal sites (OMSs). Such OMSs are expected to work as Lewis acidic centers and also as interaction sites for gas molecules through charge-transfer (CT) and electrostatic (ES) interactions. Typical OMSs are found in the MOF-74 (or CPO-27) series.[12,13] Experimental and theoretical studies showed that the large adsorption energies of gas molecules arise from the presence of OMSs.[14−24] The HKUST-1 series are other well-known PCPs possessing OMSs.[25−31] In these PCPs, OMS is the Cu center of a paddle-wheel unit that consists of binuclear metal ions and four carboxylate ligands; this OMS is called Cu-OMS hereafter. As expected, the OMS interacts with guest gas molecules; for example, several experimental studies reported that gas molecules such as CH_4,[32,33] C_2H_2,[34] CO,[35−37] CO_2,[37,38] N_2,[38] H_2,[39] and MeCN[40] interact with the Cu-OMS. The interaction was discussed in terms of σ-donation and π-back-donation in the HKUST-1 based on the shift of the IR frequency. Theoretical calculations were also carried out to investigate the effects of the Cu-OMS on gas adsorption and the nature of the interaction between the Cu-OMS and the gas molecules.[41−45] Some studies suggested that the ES interaction is important for the adsorption energy.[44−46] In contrast, several other papers suggested that the orbital interaction between the Cu-OMS and gas molecules is important for gas adsorption.[47−53] This unclear situation about the interaction for gas adsorption stimulated us to perform a systematic and comprehensive theoretical study of the interaction between the Cu-OMS and gas molecules. Such theoretical knowledge is

Received: August 26, 2013
Published: February 10, 2014

   dx.doi.org/10.1021/ic402172v | Inorg. Chem. 2014, 53, 2417−2426

indispensable for better understanding gas adsorption on PCPs and designing PCPs for selective adsorption of gas molecules.

In this work, we theoretically investigated the interactions between the Cu-OMS and various gas molecules such as MeNC, MeCN, H_2O, C_2H_4, C_2H_2, CO, CO_2, N_2, CH_4, and H_2. Some of these are targets for gas storage and/or gas separation. Our purposes here are to evaluate the binding energy (E_b) of the gas molecule, to reveal the nature of the interaction between the gas molecule and Cu-OMS, and to clarify the reason why the stretching frequency is shifted by interaction with the Cu-OMS. The frequency shift is one of the observable properties in experiments to inform us how strongly a gas molecule interacts with the OMS and how much they are activated/stabilized. Hence, a theoretical knowledge of the relationship between the frequency shift and nature of the interaction is indispensable to understand gas adsorption and gas separation by PCPs/MOFs.

COMPUTATIONAL DETAILS AND MODELS

We adopted the model systems shown in Scheme 1. Although the whole structure of the PCP[54] and some of the PCP[55] were considered

Scheme 1. Model of a Cu Paddle-Wheel Unit with a Gas Molecule (L), Where R = H (1-L), Me (2-L), or Ph (3-L)

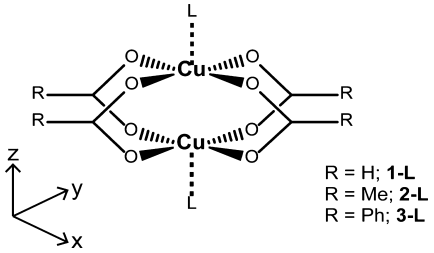

in previous theoretical studies, we employed here only the Cu-OMS part as the first step of this series of study. The simplest model $[Cu_2(O_2CH)_4]$ (**1**) is constructed from two Cu^{2+} metals and four formate ligands. Axial positions are occupied by various gas molecules (L). Hereafter, we denote them as **1-L** to represent the system $[Cu_2(O_2CH)_4](L)_2$ consisting of the Cu paddle-wheel unit and two L molecules. We also employed Cu paddle-wheel units consisting of acetate and benzoate ligands to investigate the effect of the carboxylate group on the E_b of L. The acetate and benzoate complexes are named $[Cu_2(O_2CMe)_4]$ (**2**) and $[Cu_2(O_2CPh)_4]$ (**3**), respectively.

All geometry optimizations were carried out using the density functional theory (DFT) method with the M06L functional.[56] For Cu, a (311111/22111/411/11) basis set including two f polarization functions was used, where the core electrons were replaced with the effective core potentials of the Stuttgart–Dresden–Bonn group.[57] The 6-311G(2d) basis sets were employed for all gas molecules except for the H_2 molecule. The 6-311G(2d,2p) basis set was employed for the H_2 molecule. The 6-311G(d) basis sets were used for the other atoms, where one set of anion functions was added to the O of carboxylate. Geometry optimization, frequency calculation, and population analysis were carried out with the *Gaussian 09* program package.[58] In general, the frequency calculated using DFT is overestimated. However, we did not employ a scaling factor here because it has not been reported for the M06L functional. The relative values of the frequency shift can be reasonably discussed without the scaling factor. Natural bond orbital (NBO) atomic charge is employed for the discussion. The CASSCF/MRMP2 calculations and localized molecular orbital (LMO) energy decomposition analysis[59] were performed using the *GAMESS* package.[60]

Because the Cu-OMS consists of two Cu centers with d^9 electron configurations, the dinuclear Cu^{II} paddle-wheel unit takes either an open-shell singlet or triplet state in the ground state. Thus, we investigated the relative stabilities of the two spin states with the DFT and MRMP2 methods.

The binding energies of L were evaluated using the M06L, MP2–MP4(SDQ), and SCS–MP2 methods. The E_b is defined by eq 1:

$$E_{b,L} = [E_{Cu\text{-}L} - (E_{Cu} + 2E_L)]/2 \quad (1)$$

where $E_{Cu\text{-}L}$ is the total energy of the optimized Cu paddle-wheel unit coordinating with L, E_{Cu} is the total energy of the optimized Cu paddle-wheel units without L, and E_L is the total energy of the optimized L molecule. In other words, $E_{b,L}$ represents the binding energy per L molecule. The basis set superposition error (BSSE) was corrected using the counterpoise method.[61] We examined what method provides reliable binding energies of various gas molecules because the $E_{b,CO}$ values are sensitive to the computational method, as shown in Table S1 in the Supporting Information (SI). As will be discussed in the next section, the M06L-calculated binding energies of C_2H_2 and H_2 with **3** agree with the experimental values, and that of CH_4 is slightly smaller than the experimental value. The ONIOM-(MP4(SDQ):M06L)-calculated[62] binding energies of C_2H_2 and H_2 are somewhat smaller than the experimental values. Considering these results, we hereafter employed DFT with the M06L functional for evaluating E_b.

In the CASSCF/MRMP2 calculation, 18 electrons in 10 orbitals are considered in the active space in which all d orbitals of the Cu atoms were considered. The E_b of CO calculated by CASSCF/MRMP2 is defined by eqs 2 and 3:[63]

$$E_{b,CO,CASSCF} = [E_{Cu\text{-}CO,CASSCF} - (E_{Cu,CASSCF} + 2E_{CO,HF})]/2 \quad (2)$$

$$E_{b,CO,MRMP2} = [E_{Cu\text{-}CO,MRMP2} - (E_{Cu,MRMP2} + 2E_{CO,MP2})]/2 \quad (3)$$

BSSE was not corrected in this case because CASSCF/MRMP2 was used to investigate the relative stabilities of the open-shell singlet and triplet states.

RESULTS AND DISCUSSION

Difference in Geometry between Singlet and Triplet States. The Cu^{II} center takes a d^9 electron configuration with a doublet spin state. Because one paddle-wheel unit consists of two Cu^{II} centers and four carboxylate anions, there are two possible spin states, triplet and open-shell singlet states. In general, the open-shell singlet is more stable than the triplet state at low temperature, but the triplet is observed at room temperature in many cases. Here, we investigated how much the geometry and the binding energy differ between these two spin states.

The geometries of **1** and $[Cu_2(O_2CH)_4](CO)_2$ (**1-CO**) in the triplet state were optimized using the DFT method with the M06L functional, and their geometries in the open-shell singlet state were optimized by the broken-symmetry DFT method with the same functional (Scheme 2). The structures of **1** in both the open-shell singlet and triplet states are essentially the same, as shown in Figure 1. The Cu–O distances in **1-CO** are moderately larger than those in **1**, and the Cu–Cu distances are larger in **1-CO** than in **1** by ca. 0.1 Å in both spin states. The Cu–CO distances are slightly different between the two states: 2.256 Å in the open-shell singlet and 2.267 Å in the triplet state.

The MRMP2 method usually provides a reliable energy difference between open-shell singlet and triplet states. The open-shell singlet is calculated to be more stable than the triplet state by CASSCF, MRMP2, and DFT (M06L) methods, as listed in Table 1. The energy difference calculated using MRMP2 is 2.1 kcal·mol^{-1} in **1**, which is not greatly different from the experimental value. CASSCF underestimates this energy difference, and DFT(M06L) reproduces the energy

dx.doi.org/10.1021/ic402172v | Inorg. Chem. 2014, 53, 2417–2426

Scheme 2. Schematic Description of the Electron Configurations for 1, 1-CO, and $(CO)_2$

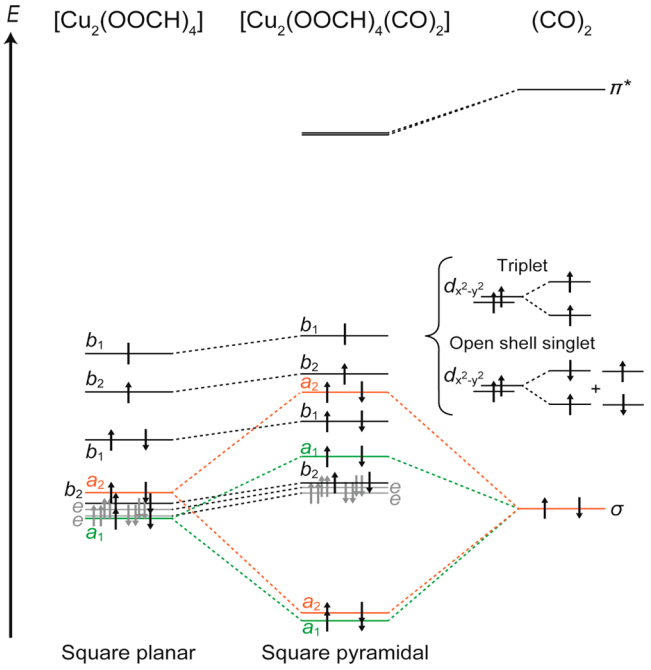

difference well. The $E_{b,CO}$ values calculated using MRMP2 are almost the same between the open-shell singlet and triplet states, as shown in Table 1. The $E_{b,CO}$ values calculated using M06L are the same in these two states. Other computational methods also provide similar $E_{b,CO}$ values in these two spin states, as shown in Table S1 in the SI.

On the basis of the above results, we concluded that the geometry and binding energy of **1-CO** are almost the same between the open-shell singlet and triplet states and that the $E_{b,CO}$ in the triplet state can be employed to investigate the relative strength of the interaction between gas molecules and the Cu-OMS. These conclusions are considered reasonable as follows: the presence of two singly occupied $d_{x^2-y^2}$ orbitals is the origin of the open-shell singlet and triplet spin states. These two states arise from different combinations of the two singly occupied $d_{x^2-y^2}$ orbitals. However, the $d_{x^2-y^2}$ orbitals do not directly overlap with the CO lone-pair orbitals. Hence, the relative energy of the open-shell singlet and triplet states is little influenced by CO coordination, and the $E_{b,CO}$ depends little on the spin state.

Table 1. Energy Differences of 1 and 1-CO between the Two Spin States and $E_{b,CO}$ in Each Spin State

	$E_{b,CO}$[a]/kcal·mol^{-1}		$\Delta E_{T\text{-}OS}$[b]/kcal·mol^{-1}	
method	open-shell singlet	triplet	**1**	**1-CO**
M06L	8.1	8.1	+2.4	+2.4
CASSCF	5.8	5.7	+0.26	+0.07
MRMP2	12.2	13.1	+2.1	+0.3
exptl[c]			+1.3	

[a]Counterpoise correction was made except for the results of CASSCF and MRMP2. [b]$\Delta E_{T\text{-}OS} = E_{\text{triplet state}} - E_{\text{open-shell singlet state}}$. [c]This experimental value refers to an anhydrous framework, MOF-11, consisting of an adamantane tetracarboxylate paddle-wheel.[76]

Effect of the Carboxylate Ligand on the Binding Energy. We investigated the E_b for three kinds of carboxylate ligands. The optimized Cu−O distances are little different in **1**−**3**, while the Cu−Cu distance moderately decreases in the order **1** > **2** > **3**, as shown in Figure 1. The same trend is observed in **1-CO**, **2-CO**, and **3-CO**. In contrast, the Cu−CO distance moderately increases in the reverse order, **1-CO** < **2-CO** < **3-CO**. The $E_{b,CO}$ calculated using M06L moderately decreases in the order **1-CO** (8.1 kcal·mol^{-1}) > **2-CO** (7.2 kcal·mol^{-1}) > **3-CO** (6.8 kcal·mol^{-1}), as shown in Table S2 in the SI.

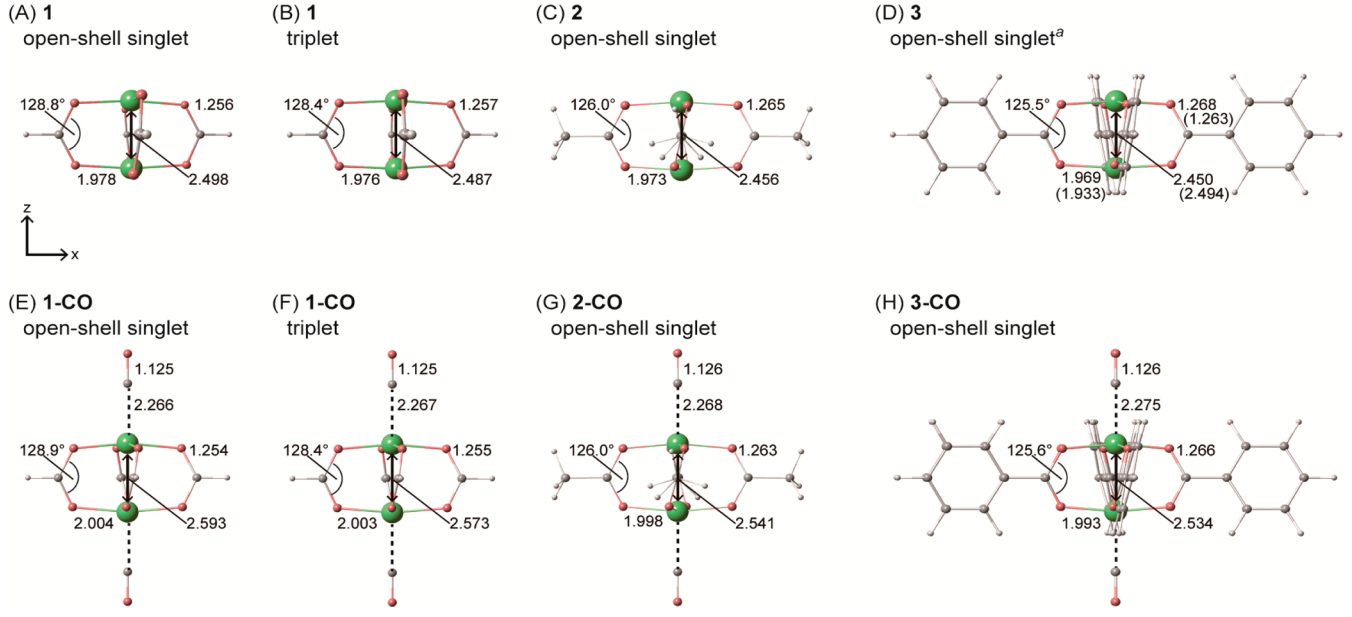

Figure 1. Optimized structures of **1**−**3**, **1-CO**, $[Cu_2(O_2CMe)_4](CO)_2$ (**2-CO**), and $[Cu_2(O_2CPh)_4](CO)_2$ (**3-CO**). The distances are in angstroms. Experimental values are shown in parentheses.[64] Green, red, gray, and white spheres show Cu, O, C, and H atoms, respectively. D_2 symmetry was employed in parts C and G, and D_4 symmetry was employed in the others. [a]Because the X-ray structure was measured at 100 K,[64] where the framework is in the open-shell singlet,[75] we calculated the open-shell singlet.

dx.doi.org/10.1021/ic402172v | Inorg. Chem. 2014, 53, 2417−2426

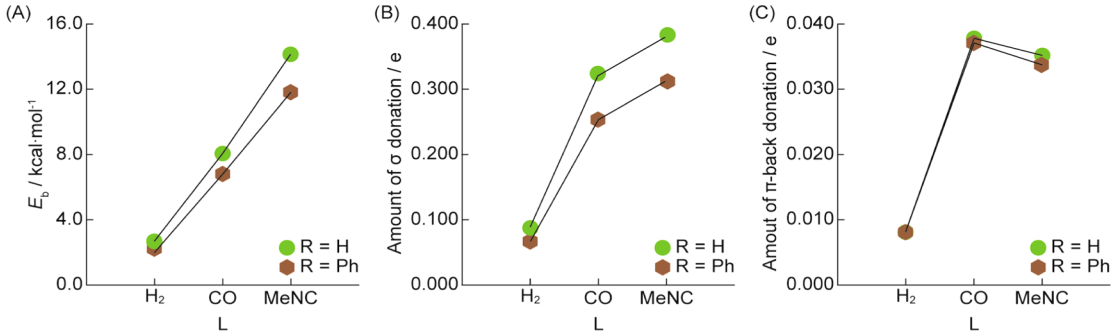

Figure 2. Dependence of (A) E_b, (B) σ-donation, and (C) π-back-donation of H_2, CO, and MeNC on the kinds of carboxylate group (HCO_2^- and $PhCO_2^-$).

The model of **3** is the basic model of building units consisting of aromatic carboxylates. We compared the optimized structures of **3** with the experimental structures of HKUST-1 in the degassed phase.[64] The Cu−Cu, Cu−O, and C−O distances in the carboxylates agree well with the experimental values, as shown Figure 1.

We also investigated the interactions of MeNC and H_2 with **1** and **3**. MeNC was selected as a strongly coordinating molecule and H_2 as a weakly coordinating molecule. The optimized structures of **1-H$_2$**, **3-H$_2$**, **1-MeNC**, and **3-MeNC** are shown in Figure S1 in the SI. The dependencies of E_b, the strength of σ-donation, and that of π-back-donation on L = H_2, CO, and MeNC are similar between **1** and **3**, as shown in Figure 2.[65−69] These results suggest that **1** is a reasonable model for discussing the relative strength of the interaction between gas molecules and the Cu-OMS.

Geometries and Binding Energies of Various Gas Molecules with 1. We will inspect the geometry changes caused by CO coordination. As shown in Figure 1, CO coordination induces elongation of the Cu−Cu distance by ca. 0.1 Å and the Cu−O distances by ca. 0.02 Å in all three complexes. We inspected several important orbital interactions that may induce elongation of the Cu−Cu distance. However, σ-donation from CO to the unoccupied molecular orbitals (MOs) of [$Cu_2(O_2CH)_4$] does not explain the elongation. The π-back-donation from Cu to CO is very weak in this complex, which is also not responsible for the elongation; see the SI, page S3. At this moment, we could not find the reason, and we have to continue efforts to find the reason for this Cu−Cu distance elongation.

We investigated the interactions between **1** and gas molecules such as MeNC, H_2O, MeCN, C_2H_4, C_2H_2, CO, CO_2, N_2, CH_4, and H_2 in the triplet state because the difference in E_b between the triplet and open-shell singlet states is quite small, as was discussed above. In **1-H$_2$O** and **1-CO$_2$**, their O atoms take positions deviating from the z axis, as shown in Figure 3, although the O atoms of H_2O and CO_2 have lone-pair orbitals that mainly participate in coordination with the metal center. This is probably because the positively charged H atoms of H_2O and the positively charged C atom of CO_2 interact with the negatively charged O atoms of the carboxylate. In **1-CH$_4$**, the C−H σ-bonding orbital interacts with the Cu atom as in the agostic interaction. Although the empty d orbital plays an important role in the agostic interaction in general, the Cu center has no empty d orbital extending toward the CH_4 molecule. Instead of the 3d orbital, the empty 4p_z orbital of the Cu center participates in the agostic interaction. The C atom takes a position deviating from the z axis to produce a good overlap between the σ-bonding orbital of CH_4 and the empty 4p_z orbital of the Cu center. MeNC, MeCN, and N_2 exist on the z axis with an end-on coordination form. In contrast, C_2H_4, C_2H_2, and H_2 take the side-on coordination form, in which the centers of the C−C and H−H bonds lie on the z axis. The CH_2 plane in **1-C$_2$H$_4$** is moderately bent back by interaction with the Cu center, and the H−C−C angle in **1-C$_2$H$_2$** also becomes moderately smaller than 180°. These geometrical features are often observed in many alkene and alkyne metal complexes, as has been discussed as the Dewar−Chatt−Duncanson model in previous studies.[70,71] The Cu−Cu distances are elongated by coordination of the gas molecules in all of these complexes, the reason for which is not clear. The E_b decreases in the order MeNC > H_2O > MeCN > C_2H_4 > C_2H_2 > CO > CO_2 > N_2 > CH_4 > H_2 in both MP4(SDQ) and M06L computational results, as summarized in Table 2. The next issue to be discussed is, what are the determining factors for the E_b?

Determining Factors for the Binding Energy of Gas Molecules with 1. We will discuss here the E_b at the Hartree−Fock (HF) level and at the MP2 level. This analysis is reasonable as follows: Because the Moller−Plesset perturbation theory provides reliable binding energy of gas molecule with PCP, the HF wave function is a good approximation, and hence the binding energy can be discussed by separating it to that at the HF level and that by the correlation effect. The E_b at the HF level is analyzed with LMO energy decomposition analysis, which can be applied to open-shell systems.[59] The ES provides significantly high stabilization, while the EX gives rise to significantly high destabilization, as shown in Table 3. The plot of the ES term against the total E_b shows a linear relationship, while the EX term also exhibits a negative linear relationship against the total E_b, as shown in Figure 4A,B. Because these two relationships are the reverse of each other, ES stabilization is almost compensated for by EX destabilization, as shown in Figure S2A in the SI. The sum of ES and EX, which corresponds to the static energy, has little influence on the trend of E_b. The CT + polarization (Pol) with other mixing terms (CT+Pol) also shows a linear relationship against the total E_b, as shown in Figure 4C. The correlation energy does not apparently exhibit any clear relationship with the total E_b, as shown in Figure 4D, indicating that the correlation effect is not a crucial factor in determining the trend of E_b. These results suggest that the CT+Pol term plays an important role in determining the trend of E_b of gas molecules with **1**.

We also investigated the relationship between the frontier orbital energy and stabilization energy of the CT+Pol term. A positive relationship is observed except for CH_4, C_2H_4, and C_2H_2, as shown in Figure S2B in the SI, in which the CT+Pol

dx.doi.org/10.1021/ic402172v | Inorg. Chem. 2014, 53, 2417−2426

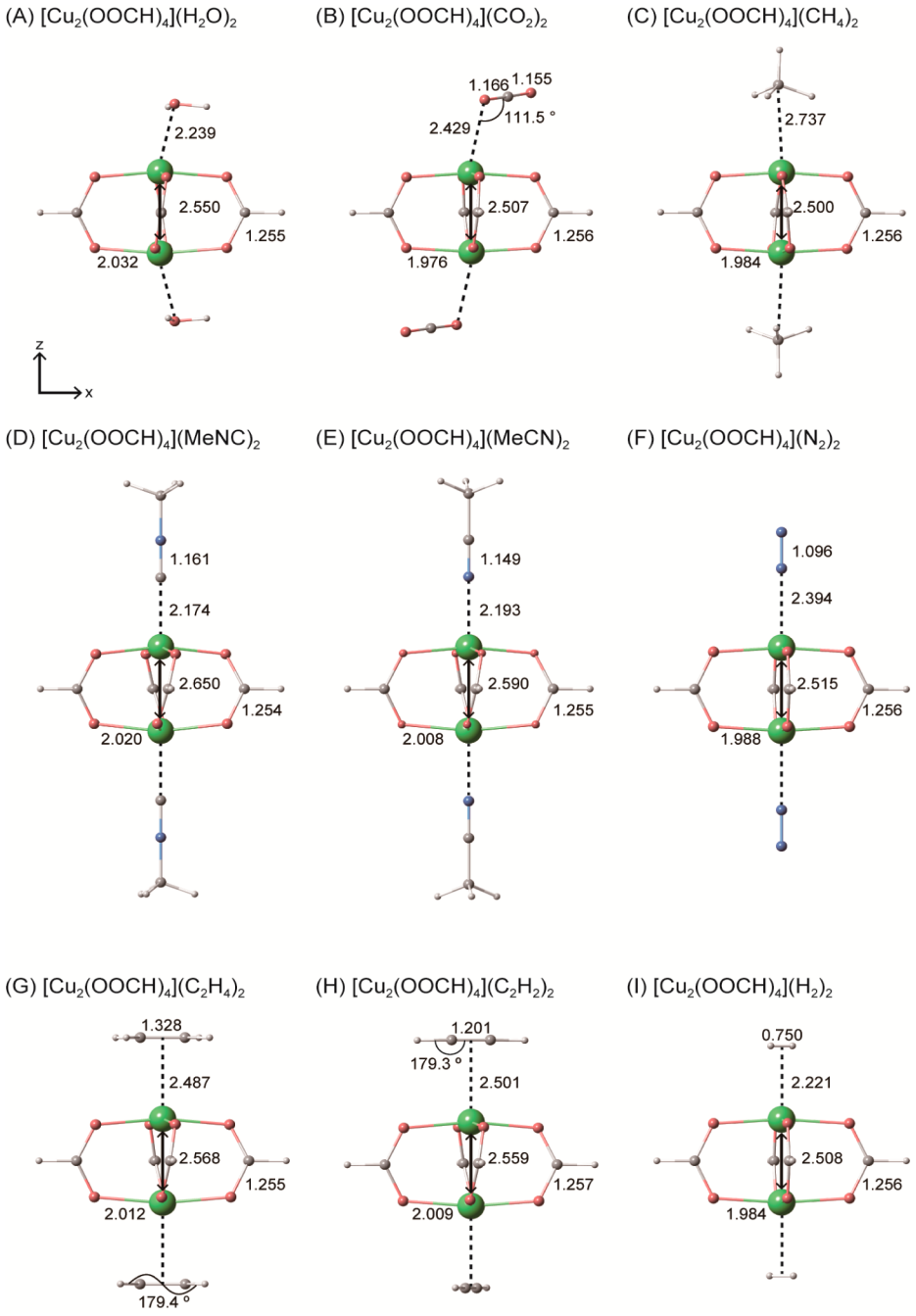

Figure 3. Optimized structures of $[Cu_2(O_2CH)_4](L)_2$ (L = H_2O, CO_2, CH_4, MeNC, MeCN, N_2, C_2H_4, C_2H_2, and H_2) in the triplet state. Distances are in angstroms. Green, red, gray, blue, and white spheres show Cu, O, C, N, and H atoms, respectively.

term moderately deviates from a linear relationship. This exception arises from the difference in the orbital. The π orbitals of C_2H_4 and C_2H_2 overlap less with the $4p_z$ orbital of the Cu center than the σ lone-pair orbitals of MeNC, MeCN, and CO. As a result, CT+Pol stabilization becomes smaller in these complexes than expected from the orbital energy. In CH_4, CT+Pol stabilization becomes much smaller than expected because the C−H σ-bonding orbital overlaps the least with the $4p_z$ orbital of the Cu center. From these results, we conclude that when the frontier orbital exists at higher energy, CT+Pol interaction becomes stronger and the E_b becomes larger.

Shift of the Stretching Frequency of Gas Molecules by Coordination. One of the experimental observations is that CO and N_2 molecules interacting with the Cu-OMS exhibit a shift to higher stretching frequency, and H_2 and CO_2 molecules exhibit a shift to lower frequency.[35,38,72] These frequency shifts are recognized as an observable property, indicating that the gas molecule interacts with the Cu-OMS. It is essential to elucidate the reason why the frequency shift is induced because knowledge of the reason provides us information to analyze and better understand the interaction between gas molecules and OMSs. Our calculations show shifts to higher stretching frequency in **1-MeNC**, **1-CO**, **1-MeCN**, and **1-N_2** and to lower frequency in **1-C_2H_4**, **1-C_2H_2**, **1-H_2**, and **1-CO_2**, as shown in Table 3. The shifts to higher frequency in CO and N_2 and to lower frequency in H_2 and CO_2 agree with the experimental results.[35,38,72] Although the calculated absolute values of the frequencies are somewhat different from the experimental

dx.doi.org/10.1021/ic402172v | Inorg. Chem. 2014, 53, 2417−2426

Table 2. Binding Energy (E_b) of the Gas Molecule L (L = MeNC, H_2O, MeCN, C_2H_2, C_2H_4, CO, CO_2, N_2, CH_4, and H_2) with 1 and 3 Calculated Using the MP4, M06L, and ONIOM Methods

	E_b[a]/kcal·mol^{-1}				
	1-L		3-L		
L	MP4(SDQ)	M06L	M06L	ONIOM[b]	exptl
MeNC	13.4	14.1			
H_2O	12.2	13.1			
MeCN	11.4	11.4			
C_2H_4	7.6	9.5			
C_2H_2	6.9	8.5	7.4	5.8	7.3[34]
CO	5.8	8.1			
CO_2	4.8	5.4			
N_2	3.4	4.0			
CH_4	2.2	3.7	3.3	1.8	4.3[32]
H_2	1.6	2.6	2.2	1.2	1.6[77]

[a]Counterpoise correction was made. [b]ONIOM [MP4(SDQ)/M06L].

values, the shift values and their trends are not greatly different between the calculated and experimental values. These results suggest that the present computational values are useful for analyzing the frequency shift.

The shift to higher frequency of the CO stretching frequency was previously explained in terms of the C−O bond polarization by the presence of a positive charge in the lone-pair region.[73,74] A similar examination, however, has not been made for other gas molecules such as N_2, MeCN, and MeNC. We placed a positive charge (q = 0.0−1.2 e) at the same position as the Cu center and evaluated how much the frequency is shifted by the positive charge. Certainly, the presence of the positive charge induces a considerably higher shift in CO and MeNC and moderately higher shift in N_2 and MeCN, as shown in Figure 5 and Table S5 in the SI. Linear relationships are observed between the frequency shift and the size of the point charge. The slopes are much larger in CO and MeNC than in N_2 and MeCN. In N_2 and MeNC, the frequency moderately increases when the positive charge increases to q = 0.3−0.4 e and increases little when the positive charge increases from q = 0.5 to 1.2 e.

The frequency shifts caused by a positive charge were larger than the calculated values for **1-L** (L = MeNC, CO, and N_2) when the Cu atomic charge calculated in **1-L** was placed at the Cu position, as shown in Table 3. This discrepancy arises from the presence of the negative charge on the O atom in the carboxylate moiety. We calculated the frequency shift with point charges corresponding to $[Cu_2(O_2CH)_4]$. The shift values are not greatly different from those calculated in **1-L**. These results suggest that the frequency shift is induced by the charge distribution of the $[Cu_2(O_2CH)_4]$ moiety in these end-on-coordinated gas molecules.

In the side-on-coordinated C_2H_4, C_2H_2, and H_2 molecules, a shift to lower frequency is often observed experimentally. Such a shift was explained by the CT interactions, such as donation and back-donation interactions. However, the presence of a positive charge clearly induces a shift to lower frequencies, as shown in Figure 5A. The shift by a positive charge is significantly larger in H_2 than in C_2H_2 and C_2H_4 because the reduced mass is quite small in H_2; a small change of the force constant in H_2 produces a large change in the frequency. In other words, the frequency is much more sensitive to the force constant in H_2 than in C_2H_2 and C_2H_4. The extent of the shift becomes smaller than the calculated value for **1-L**, when the atomic charges corresponding to $[Cu_2(O_2CH)_4]$ are used, as shown in Table 3. This behavior is different from that of the end-on-coordinated gas molecules. These features suggest that not only the charge distribution but also some other factors, such as CT interactions, contribute to the shift to lower frequency in the side-on-coordinated form.

CO_2 molecules take neither a pure end-on-coordinated nor a pure side-on-coordinated form, as shown in Figure 3B. When the positive charge is placed at the same position as the Cu center, a lower frequency shift is induced by the charge, where the angle of Cu−O−C (θ) is 111.5°. This lower shift is interesting because a lower shift is not observed very often in the η^1-end-on structure.[38] When the Cu atomic charge in **1-CO_2** is used, a lower shift is induced, as in **1-CO_2**. However, a higher shift is induced when the charge distribution corresponding to $[Cu_2(O_2CH)_4]$ is used, as shown in Table 3. The shift also depends on θ, as shown in Figure 5B. The most negative shift is calculated at θ = 90° and the most positive shift at θ = 180°, which corresponds to a pure end-on structure. These results suggest that the frequency shift of CO_2 is sensitive to the charge distribution of the PCP and the orientation of the CO_2 molecule in the PCP.

We summarized here the above discussion as follows: (i) the frequency shift of a gas molecule depends not only on the CT interaction but also on the ES potential, when the gas molecule forms an η^1-end-on interaction with the Cu-OMS, (ii) the

Table 3. Frequency (ν) of L (L = MeNC, CO, MeCN, N_2, C_2H_4, C_2H_2, H_2, and CO_2) with Charges and Their Shifts ($\Delta\nu$) Relative to the Frequency of Free L

	L							
frequency ν/cm^{-1}	MeNC	CO	MeCN	N_2	C_2H_4	C_2H_2	H_2	CO_2
exptl free L[38]		2143		2330			4160	2349
exptl L in the PCP[38]		2179		2334			4090	2330
exptl $\Delta\nu$		+36		+4			−70	−19
calcd free L	2213.9	2194.6	2342.3	2397.1	1704.6	2064.5	4323.8	2478.3
calcd **1-L**	2277.0	2228.8	2380.4	2407.7	1676.1	2041.8	4226.5	2466.3
calcd $\Delta\nu$	+63.1	+34.2	+38.1	+10.6	−28.5	−22.7	−97.3	−12.0
L with Cu atomic charge[a]	2314.8	2270.5	2369.7	2410.4	1680.9	2042.8	4252.1	2472.0
$\Delta\nu$	+100.9	+75.9	+27.4	+13.3	−23.7	−21.7	−71.7	−6.3
L with charge distribution of **1**[a]	2277.8	2234.4	2370.4	2410.7	1692.1	2057.7	4278.6	2481.4
$\Delta\nu$	+63.9	+39.8	+28.1	+13.6	−12.5	−6.8	−44.9	+3.1

[a]NBO atomic charges in **1-L** are used, as shown in Scheme S1 in the SI.

dx.doi.org/10.1021/ic402172v | Inorg. Chem. 2014, 53, 2417−2426

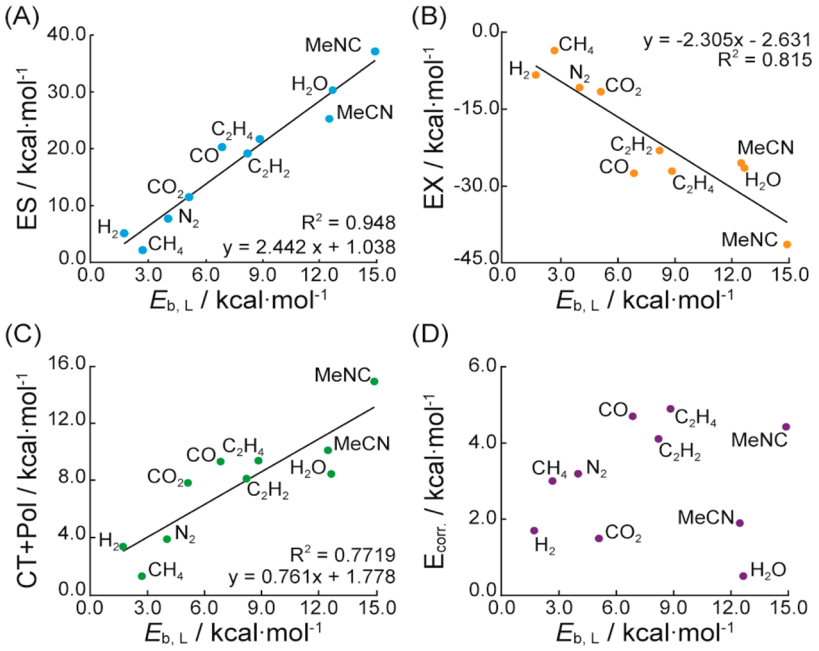

Figure 4. (A) ES interaction energy versus total binding energy, (B) exchange repulsion interaction energy (EX) versus total binding energy, (C) sum of the CT, polarization, and other interaction energy (CT+Pol) versus total binding energy, and (D) correlation energy versus total binding energy. Positive and negative values indicate stabilization and destabilization, respectively.

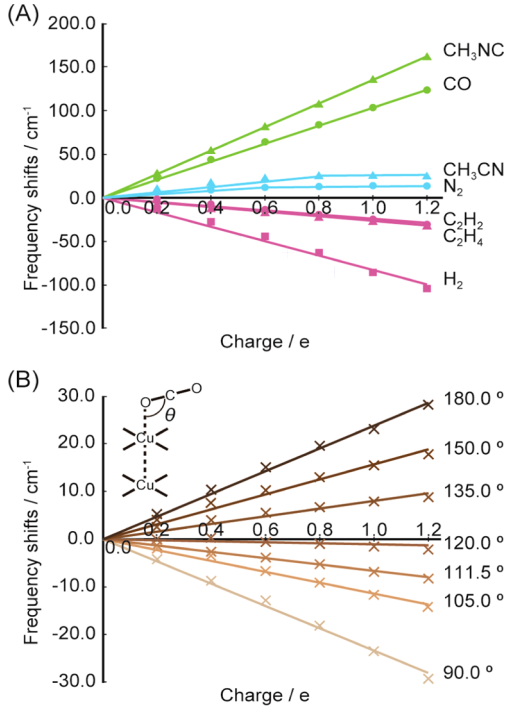

Figure 5. (A) Frequency shifts of gas molecules L (L = H_2O, CH_4, MeNC, MeCN, N_2, C_2H_4, C_2H_2, and H_2) by a positive charge (q = 0.0−1.2 e) and (B) frequency shifts of CO_2 at various orientations against the Cu−Cu axis (θ = 90.0−180.0°).

frequency shift provides us the information about the CT interaction when the gas molecule interacts with the Cu-OMS in an η^2-side-on form, and (iii) the frequency shift should be discussed in terms of the ES potential when the gas molecule does not interact with the Cu-OMS.

How Much Does the Positive Charge Influence the Electronic Structure of the Gas Molecule? We evaluated how much the distribution of the electron density is influenced by the positive charge, where the difference in the total electron density is named $\Delta\rho_t$ and the density changes in the lone-pair, σ, and π orbitals are named $\Delta\rho_{lp}$, $\Delta\rho_\sigma$, and $\Delta\rho_\pi$, respectively.

In CO, the total electron density is withdrawn toward the positive charge and the density increases in the C−O bonding region, as shown in Figure 6A, where a positive charge is placed at the same position as the Cu center. The sum of $\Delta\rho_{lp}(\varphi_7)$ and $\Delta\rho_\sigma(\varphi_4)$ indicates a moderate decrease in the bonding region, and both $\Delta\rho_\pi(\varphi_5)$ and $\Delta\rho_\pi(\varphi_6)$ show an increase in the bonding region. The electron density of MeNC changes in a manner similar to that of CO, as shown in Figure S3A in the SI.

On the other hand, the change in the total density is much smaller in N_2 and MeCN than in CO and MeNC, as shown in Figures 6B and S3B in the SI. These smaller changes correspond to the moderate frequency shift calculated for N_2 and MeCN. $\Delta\rho_{lp}(\varphi_7)$, $\Delta\rho_\pi(\varphi_5)$, and $\Delta\rho_\pi(\varphi_6)$ show that the density increases around the N atom near the positive charge and decreases around the N atom distant from the positive charge in the N−N bonding region. Although the sum of the density changes in $\Delta\rho_{lp}(\varphi_7)$ and $\Delta\rho_\sigma(\varphi_4)$ slightly decreases in the N−N bonding region, the increase of the electron density in the π orbitals contributes to the increase of $\Delta\rho_t$ around the N atom near the positive charge. As a result, $\Delta\rho_t$ exhibits a node in the N−N bonding region, which is the origin of the moderate density change in the bonding region. The electron density is similarly changed in MeCN by the positive charge, as shown in Figure S3B in the SI. These results indicate that the frequency shift closely relates to the change in the electron density caused by the positive charge.

The density change depends on the extent of polarization induced by a positive charge. The z component of the polarizability (z polarizability) increases in the order MeCN (2.07 Å^3) ~ N_2 (2.09 Å^3) < CO (5.46 Å^3) < MeNC (5.92 Å^3), where the z polarizability calculated with the M06L functional is in parentheses. This order agrees with the extent of the

dx.doi.org/10.1021/ic402172v | Inorg. Chem. 2014, 53, 2417−2426

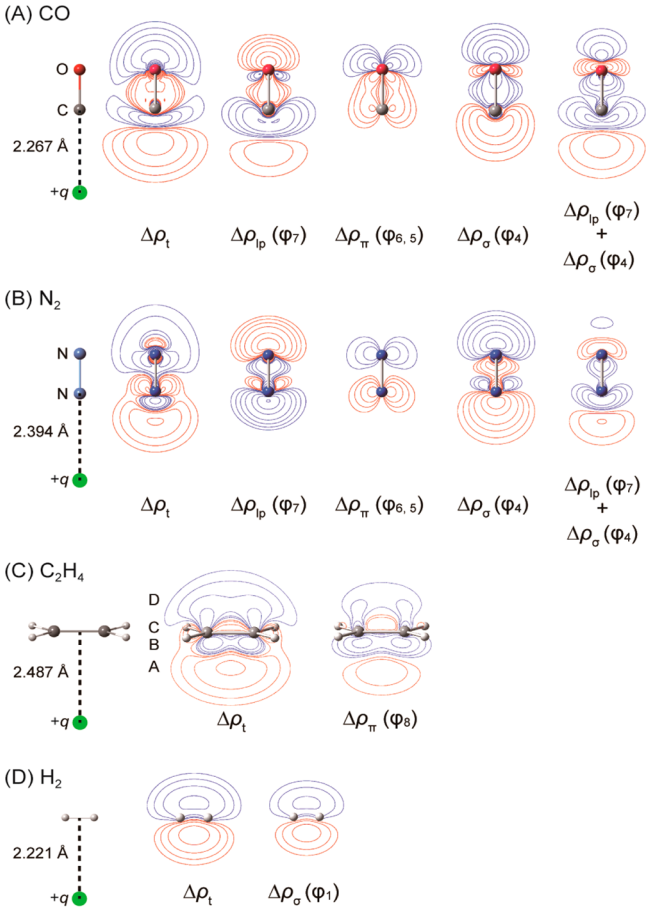

Figure 6. Contour lines of the change in the electron density induced by a positive charge ($\Delta\rho_t = \rho_t^q - \rho_t^0$, $\Delta\rho_{lp} = \rho_{lp}^q - \rho_{lp}^0$, $\Delta\rho_\sigma = \rho_\sigma^q - \rho_\sigma^0$, and $\Delta\rho_\pi = \rho_\pi^q - \rho_\pi^0$), where q = 1.2 e. Blue and orange lines indicate a decrease and an increase in the electron density, respectively. Red, gray, blue, and white spheres show O, C, N, and H atoms, respectively.

frequency shift except for the order between MeCN and N_2, indicating that the frequency shift by the positive charge is mainly determined by the z polarizability. We examined the orbital energies of the lone-pair and π^* orbitals, as shown in Table S6 in the SI, because polarization occurs more easily when the energy gap is small between occupied and unoccupied orbitals. As expected, the energy gap is larger in MeCN and N_2 than in CO and MeNC and decreases in the order MeCN (8.96 eV) ∼ N_2 (8.95 eV) > CO (7.79 eV) > MeNC (7.37 eV), where the energy gaps calculated with M06L are in parentheses. The order is consistent with the order of the z polarizability except for the small difference between MeCN and N_2. This result indicates that the lone-pair and π^* orbitals play important roles in the polarizability and, hence, the frequency shift.

In C_2H_4, C_2H_2, and H_2, which take the side-on-coordinated form, the total electron density increases in the A area near the positive charge and decreases in the B area distant from the positive charge; see Figure 6C for the A and B areas and Figures 6D and S3C in the SI. As a result, the density changes little between the two C atoms in C_2H_4 and C_2H_2 and the two H atoms in H_2, even when the positive charge is placed at the same position as the Cu atom. As discussed above, the charge distribution of $[Cu_2(O_2CH)_4]$ induces a much smaller shift than the calculated values in **1**-C_2H_4, **1**-C_2H_2, and **1**-H_2. These results indicate that not only the polarization induced by charges but also the CT interaction contribute to the frequency shift.

The electron population actually decreases in the π orbital and increases in the π^* orbital in both **1**-C_2H_4 and **1**-C_2H_2, as shown in Table 4.[78] The electron population of the σ-bonding orbital also decreases in **1**-H_2. These population changes contribute to the lower frequency shift. We conclude that the CT interaction actually induces the lower frequency shift in these molecules.

CONCLUSION

We theoretically evaluated the E_b between various gas molecules and Cu paddle-wheel units, $[Cu_2(O_2CR)_4]$ (R = H, Me, or Ph), where $[Cu_2(O_2CR)_4]$ was employed as a model of a typical Cu-OMS. The DFT(M06L)-optimized geometry of **3** agrees with the experimental structure of the PCP bearing Cu-OMS. The $E_{b,CO}$ in **1-CO** is only slightly different between the open-shell singlet and triplet states, and thus the E_b values of various gas molecules were evaluated with the M06L and MP4(SDQ) methods in the triplet state. The E_b decreases in the order MeNC > H_2O > MeCN > C_2H_4 > C_2H_2 > CO > CO_2 > N_2 > CH_4 > H_2. The LMO energy decomposition analysis at the HF level was carried out to evaluate how much the ES, EX, and CT+Pol terms contribute to E_b. A positive linear relationship is observed between the E_b and ES, while a negative linear relationship is observed between the E_b and EX. ES stabilization is almost compensated for by EX destabilization. Thus, the E_b increases with an increase in the CT+Pol. Many experimental studies claimed that the ES plays an important role in the E_b; however, our results suggest that a more careful discussion is necessary.

The stretching frequency of an adsorbed gas molecule is changed by interaction with the Cu-OMSs. The frequency shift is reproduced well by DFT calculations with the present model system **1-L**. The charge corresponding to $[Cu_2(O_2CH)_4]$

Table 4. Amount of CT between L (L = MeNC, MeCN, C_2H_4, C_2H_2, CO, NO, N_2, and H_2) and $[Cu_2(O_2CH)_4]$[a]

	L							
	MeNC	MeCN	C_2H_4	C_2H_2	CO	CO_2	N_2	H_2
NBO	0.222	0.125	0.076	0.069	0.213	0.052	0.100	0.060
NAO bond order of Cu-L	0.5254	0.3189	0.1516	0.1453	0.4743	0.1250	0.2455	0.1295
from σ orbital to metal	0.379	0.114	0.021	0.011	0.320	0.020	0.035	0.090
from π orbital to metal			0.027	0.058[b]		0.029[b,d]		
				0.014[c]		0.009[c,d]		
to π^* orbital from metal	0.033	0.015	0.018	0.014[b]	0.034	0.006[b]	0.012	0.008[e]
				0.001[c]		0.002[c]		

[a]M06L was employed. [b]π orbitals in-plane. [c]π orbitals out-of-plane. [d]Nonbonding π orbitals. [e]σ^* orbital.

dx.doi.org/10.1021/ic402172v | Inorg. Chem. 2014, 53, 2417−2426

significantly contributes to the frequency shift in the end-on-coordinated MeNC, CO, MeCN, and N_2. Although the shift is generally discussed in terms of donation and back-donation, the present result suggests that not only the CT but also the ES potential in the PCP should be considered in discussing the frequency shift. In the side-on-coordinated forms of C_2H_4, C_2H_2, and H_2, we concluded that the lower shift is induced by both the charge distribution and CT interaction.

These theoretical results clarify the role of the Cu-OMS in the interaction between gas molecules and PCPs. The present work provides detailed theoretical analyses of the binding energy of a gas molecule with the Cu-OMS and the frequency shift of the gas molecule by interaction with the Cu-OMS. We believe that our results are essential for discussing gas adsorption and their frequency shifts.

■ ASSOCIATED CONTENT

Supporting Information

$E_{b,CO}$ depending on functionals, E_b, and theoretically analyzed values of CO, H_2, and MeNC depending on R, optimized structures with different R for H_2, CO, and MeNC based on M06L, results of LMO energy decomposition analysis, plot of the sum of ES and EX against E_b, plot of CT+Pol against the MO energy level, frequencies of L depending on charges, charged model for calculation of frequencies, contour plots of the change in the electron density, and MO energy levels of L. This material is available free of charge via the Internet at http://pubs.acs.org.

■ AUTHOR INFORMATION

Corresponding Author

*E-mail: sakaki.shigeyoshi.47e@st.kyoto-u.ac.jp.

Notes

The authors declare no competing financial interest.

■ ACKNOWLEDGMENTS

This work was financially supported by a Grant-in-Aid from the Ministry of Education, Culture, Science, Sport, and Technology through the Grant-in-Aid of Specially Promoted Science and Technology (Grant 22000009). The authors thank the computer center of the Institute for Molecular Science (Okazaki, Japan) for kindly allowing use of their computers. Y.H. acknowledges the Fukui Fellowship, Kyoto University.

■ REFERENCES

(1) Kondo, M.; Yoshitomi, T.; Seki, K.; Matsuzaka, H.; Kitagawa, S. *Angew. Chem., Int. Ed.* **1997**, *36*, 1725−1727.
(2) Li, H.; Eddaoudi, M.; Groy, T. L.; Yaghi, O. M. *J. Am. Chem. Soc.* **1998**, *120*, 8571−8572.
(3) Ferey, G.; Mellot-Draznieks, C.; Serre, C.; Millange, F.; Dutour, J.; Surble, S.; Margiolaki, I. *Science* **2005**, *309*, 2040−2042.
(4) Furukawa, H.; Ko, N.; Go, Y. B.; Aratani, N.; Choi, S. B.; Choi, E.; Yazaydin, A. O.; Snurr, R. Q.; O'Keeffe, M.; Kim, J.; Yaghi, O. M. *Science* **2010**, *329*, 424−428.
(5) Deng, H.; Grunder, S.; Cordova, K. E.; Valente, C.; Furukawa, H.; Hmadeh, M.; Gándara, F.; Whalley, A. C.; Liu, Z.; Asahina, S.; Kazumori, H.; O'Keeffe, M.; Terasaki, O.; Stoddart, J. F.; Yaghi, O. M. *Science* **2012**, *336*, 1018−1023.
(6) Kitagawa, S.; Kitaura, R.; Noro, S. *Angew. Chem., Int. Ed.* **2004**, *43*, 2334−2375.
(7) Horike, S.; Shimomura, S.; Kitagawa, S. *Nat. Chem.* **2009**, *1*, 695−704.
(8) Ferey, G.; Serre, C. *Chem. Soc. Rev.* **2009**, *38*, 1380−1399.
(9) Demessence, A.; D'Alessandro, D. M.; Foo, M. L.; Long, J. R. *J. Am. Chem. Soc.* **2009**, *131*, 8784−8786.
(10) Lee, J.; Farha, O. K.; Roberts, J.; Scheidt, K. A.; Nguyen, S. T.; Hupp, J. T. *Chem. Soc. Rev.* **2009**, *38*, 1450−1459.
(11) Yoon, M.; Srirambalaji, R.; Kim, K. *Chem. Rev.* **2012**, *112*, 1196−1231.
(12) Rosi, N. L.; Kim, J.; Eddaoudi, M.; Chen, B. L.; O'Keeffe, M.; Yaghi, O. M. *J. Am. Chem. Soc.* **2005**, *127*, 1504−1518.
(13) Dietzel, P. D. C.; Morita, Y.; Blom, R.; Fjellvag, H. *Angew. Chem., Int. Ed.* **2005**, *44*, 6354−6358.
(14) Poloni, R.; Smit, B.; Neaton, J. B. *J. Phys. Chem. A* **2012**, *116*, 4957−4964.
(15) Wu, H.; Simmons, J. M.; Srinivas, G.; Zhou, W.; Yildirim, T. *J. Phys. Chem. Lett.* **2010**, *1*, 1946−1951.
(16) Dietzel, P. D. C.; Georgiev, P. A.; Eckert, J.; Blom, R.; Strassle, T.; Unruh, T. *Chem. Commun.* **2010**, *46*, 4962−4964.
(17) Rowsell, J. L. C.; Yaghi, O. M. *J. Am. Chem. Soc.* **2006**, *128*, 1304−1315.
(18) Vitillo, J. G.; Regli, L.; Chavan, S.; Ricchiardi, G.; Spoto, G.; Dietzel, P. D. C.; Bordiga, S.; Zecchina, A. *J. Am. Chem. Soc.* **2008**, *130*, 8386−8396.
(19) Zhou, W.; Wu, H.; Yildirim, T. *J. Am. Chem. Soc.* **2009**, *131*, 4995−5000.
(20) Chavan, S.; Bonino, F.; Vitillo, J. G.; Groppo, E.; Lamberti, C.; Dietzel, P. D. C.; Zecchina, A.; Bordiga, S. *Phys. Chem. Chem. Phys.* **2009**, *11*, 9811−9822.
(21) Valenzano, L.; Civalleri, B.; Chavan, S.; Palomino, G. T.; Arean, C.; Bordiga, S. *J. Phys. Chem. C* **2010**, *114*, 11185−11191.
(22) Valenzano, L.; Civalleri, B.; Sillar, K.; Sauer, J. *J. Phys. Chem. C* **2011**, *115*, 21777−21784.
(23) Park, J.; Kim, H.; Han, S. S.; Jung, Y. *J. Phys. Chem. Lett.* **2012**, *3*, 826−829.
(24) Dzubak, A. L.; Lin, L. C.; Kim, J.; Swisher, J. A.; Poloni, R.; Maximoff, S. N.; Smit, B.; Gagliardi, L. *Nat. Chem.* **2012**, *4*, 810−816.
(25) Murray, L. J.; Dinca, M.; Yano, J.; Chavan, S.; Bordiga, S.; Brown, C. M.; Long, J. R. *J. Am. Chem. Soc.* **2010**, *132*, 7856−7857.
(26) Kramer, M.; Ulrich, S. B.; Kaskel, S. *J. Mater. Chem.* **2006**, *16*, 2245−2248.
(27) Feldblyum, J. I.; Liu, M.; Gidley, D. W.; Matzger, A. J. *J. Am. Chem. Soc.* **2011**, *133*, 18257−18263.
(28) Maniam, P.; Stock, N. *Inorg. Chem.* **2011**, *50*, 5085−5097.
(29) Xie, L. H.; Liu, S. X.; Gao, C. Y.; Cao, R. G.; Cao, J. F.; Sun, C. Y.; Su, Z. M. *Inorg. Chem.* **2007**, *46*, 7782−7788.
(30) Kozachuk, O.; Yusenko, K.; Noei, H.; Wang, Y.; Walleck, S.; Glaser, T.; Fischer, R. A. *Chem. Commun.* **2011**.
(31) Chui, S. S. Y.; Lo, S. M. F.; Charmant, J. P. H.; Orpen, A. G.; Williams, I. D. *Science* **1999**, *283*, 1148−1150.
(32) Wu, H.; Simmons, J. M.; Liu, Y.; Brown, C. M.; Wang, X.-S.; Ma, S.; Peterson, V. K.; Southon, P. D.; Kepert, C. J.; Zhou, H.-C.; Yildirim, T.; Zhou, W. *Chem.—Eur. J.* **2010**, *16*, 5205−5214.
(33) Getzschmann, J.; Senkovska, I.; Wallacher, D.; Tovar, M.; Fairen-Jimenez, D.; Düren, T.; van Baten, J. M.; Krishna, R.; Kaskel, S. *Microporous Mesoporous Mater.* **2010**, *136*, 50−58.
(34) Xiang, S.; Zhou, W.; Gallegos, J. M.; Liu, Y.; Chen, B. *J. Am. Chem. Soc.* **2009**, *131*, 12415−12419.
(35) Drenchev, N.; Ivanova, E.; Mihaylov, M.; Hadjiivanov, K. *Phys. Chem. Chem. Phys.* **2010**, *12*, 6423−6427.
(36) Zou, R. Q.; Sakurai, H.; Han, S.; Zhong, R. Q.; Xu, Q. *J. Am. Chem. Soc.* **2007**, *129*, 8402−8403.
(37) Jee, B.; Petkov, P. S.; Vayssilov, G. N.; Heine, T.; Hartmann, M.; Poppl, A. *J. Phys. Chem. C* **2013**, *117*, 8231−8240.
(38) Bordiga, S.; Regli, L.; Bonino, F.; Groppo, E.; Lamberti, C.; Xiao, B.; Wheatley, P. S.; Morris, R. E.; Zecchina, A. *Phys. Chem. Chem. Phys.* **2007**, *9*, 2676−2685.
(39) Peterson, V. K.; Liu, Y.; Brown, C. M.; Kepert, C. J. *J. Am. Chem. Soc.* **2006**, *128*, 15578−15579.
(40) Jeong, N. C.; Samanta, B.; Lee, C. Y.; Farha, O. K.; Hupp, J. T. *J. Am. Chem. Soc.* **2012**, *134*, 51−54.

(41) Farrusseng, D.; Daniel, C.; Gaudillere, C.; Ravon, U.; Schuurman, Y.; Mirodatos, C.; Dubbeldam, D.; Frost, H.; Snurr, R. Q. *Langmuir* **2009**, *25*, 7383−7388.
(42) Gomez, D. A.; Combariza, A. F.; Sastre, G. *Phys. Chem. Chem. Phys.* **2012**, *14*, 2508−2517.
(43) Supronowicz, B.; Mavrandonakis, A.; Heine, T. *J. Phys. Chem. C* **2013**, *117*, 14570−14578.
(44) Babarao, R.; Jiang, J. W.; Sandler, S. I. *Langmuir* **2009**, *25*, 5239−5247.
(45) Karra, J. R.; Walton, K. S. *J. Phys. Chem. C* **2010**, *114*, 15735−15740.
(46) Zhou, C.; Cao, L.; Wei, S.; Zhang, Q.; Chen, L. *Comput. Theor. Chem.* **2011**, *976*, 153−160.
(47) Kim, Y. H.; Kang, J.; Wei, S. H. *Phys. Rev. Lett.* **2010**, *105*, 236105.
(48) Liu, D.; Zhong, C. *J. Phys. Chem. Lett.* **2009**, *1*, 97−101.
(49) Grajciar, L.; Bludsky, O.; Nachtigall, P. *J. Phys. Chem. Lett.* **2010**, *1*, 3354−3359.
(50) Watanabe, T.; Sholl, D. S. *J. Chem. Phys.* **2010**, *133*, 094509.
(51) Rubes, M.; Grajciar, L.; Bludsky, O.; Wiersum, A. D.; Llewellyn, P. L.; Nachtigall, P. *ChemPhysChem* **2012**, *13*, 488−495.
(52) Bak, J. H.; Le, V. D.; Kang, J.; Wei, S. H.; Kim, Y. H. *J. Phys. Chem. C* **2012**, *116*, 7386−7392.
(53) St. Petkov, P.; Vayssilov, G. N.; Liu, J.; Shekhah, O.; Wang, Y.; Wöll, C.; Heine, T. *ChemPhysChem* **2012**, *13*, 2025−2029.
(54) Vaidhyanathan, R.; Iremonger, S. S.; Shimizu, G. K. H.; Boyd, P. G.; Alavi, S.; Woo, T. K. *Science* **2010**, *330*, 650−653.
(55) Deshmukh, M. M.; Ohba, M.; Kitagawa, S.; Sakaki, S. *J. Am. Chem. Soc.* **2013**, *135*, 4840−4849.
(56) Zhao, Y.; Truhlar, D. G. *J. Chem. Phys.* **2006**, *125*, 19410.
(57) Dolg, M.; Wedig, U.; Stoll, H.; Preuss, H. *J. Chem. Phys.* **1987**, *86*, 866−872.
(58) Frisch, M. J.; Trucks, G. W.; Schlegel, H. B.; Scuseria, G. E.; Robb, M. A.; Cheeseman, J. R.; Scalmani, G.; Barone, V.; Mennucci, B.; Petersson, G. A.; Nakatsuji, H.; Caricato, M.; Li, X.; Hratchian, H. P.; Izmaylov, A. F.; Bloino, J.; Zheng, G.; Sonnenberg, J. L.; Hada, M.; Ehara, M.; Toyota, K.; Fukuda, R.; Hasegawa, J.; Ishida, M.; Nakajima, T.; Honda, Y.; Kitao, O.; Nakai, H.; Vreven, T.; Montgomery, J. A., Jr.; Peralta, J. E.; Ogliaro, F.; Bearpark, M.; Heyd, J. J.; Brothers, E.; Kudin, K. N.; Staroverov, V. N.; Keith, T.; Kobayashi, R.; Normand, J.; Raghavachari, K.; Rendell, A.; Burant, J. C.; Iyengar, S. S.; Tomasi, J.; Cossi, M.; Rega, N.; Millam, J. M.; Klene, M.; Knox, J. E.; Cross, J. B.; Bakken, V.; Adamo, C.; Jaramillo, J.; Gomperts, R.; Stratmann, R. E.; Yazyev, O.; Austin, A. J.; Cammi, R.; Pomelli, C.; Ochterski, J. W.; Martin, R. L.; Morokuma, K.; Zakrzewski, V. G.; Voth, G. A.; Salvador, P.; Dannenberg, J. J.; Dapprich, S.; Daniels, A. D.; Farkas, O.; Foresman, J. B.; Ortiz, J. V.; Cioslowski, J.; Fox, D. J. *Gaussian 09*, revision D.01; Gaussian, Inc.: Wallingford, CT, 2013.
(59) Li, H.; Su, P. F. *J. Chem. Phys.* **2009**, *131*, 014102.
(60) Schmidt, M. W.; Baldridge, K. K.; Boatz, J. A.; Elbert, S. T.; Gordon, M. S.; Jensen, J. H.; Koseki, S.; Matsunaga, N.; Nguyen, K. A.; Su, S. J.; Windus, T. L.; Dupuis, M.; Montgomery, J. A. *J. Comput. Chem.* **1993**, *14*, 1347−1363.
(61) Boys, S. F.; Bernardi, F. *Mol. Phys.* **1970**, *19*, 553−566.
(62) Dapprich, S.; Komaromi, I.; Byun, K. S.; Morokuma, K.; Frisch, M. J. *THEOCHEM* **1999**, *461*, 1−21.
(63) Any orbitals of CO were not considered in the active space.
(64) Wu, Y.; Kobayashi, A.; Halder, G. J.; Peterson, V. K.; Chapman, K. W.; Lock, N.; Southon, P. D.; Kepert, C. J. *Angew. Chem., Int. Ed.* **2008**, *47*, 8929−8932.
(65) Baba, H.; Suzuki, S.; Takemura, T. *J. Chem. Phys.* **1969**, *50*, 2078−2086.
(66) Fujimoto, H.; Kato, S.; Yamabe, S.; Fukui, K. *J. Chem. Phys.* **1974**, *60*, 572−578.
(67) Dapprich, S.; Frenking, G. *J. Phys. Chem.* **1995**, *99*, 9352−9362.
(68) Gorelsky, S. I. AOMix, 6.82th ed.; http://www.sg-chem.net/aomix, 2013.
(69) Gorelsky, S. I.; Lever, A. B. P. *J. Organomet. Chem.* **2002**, *659*, 202−202.
(70) Chatt, J.; Duncanson, L. A. *J. Chem. Soc.* **1953**, 2939−2947.
(71) Frenking, G. In *Modern Coordination Chemistry: The Legacy of Joseph Chatt*; Leigh, G. J., Winterton, N., Eds.; The Royal Society of Chemistry: London, 2002; pp 111−122.
(72) Prestipino, C.; Regli, L.; Vitillo, J. G.; Bonino, F.; Damin, A.; Lamberti, C.; Zecchina, A.; Solari, P. L.; Kongshaug, K. O.; Bordiga, S. *Chem. Mater.* **2006**, *18*, 1337−1346.
(73) Lupinetti, A. J.; Fau, S.; Frenking, G.; Strauss, S. H. *J. Phys. Chem. A* **1997**, *101*, 9551−9559.
(74) Goldman, A. S.; Krogh Jespersen, K. *J. Am. Chem. Soc.* **1996**, *118*, 12159−12166.
(75) Zhang, X. X.; Chui, S. S. Y.; Williams, I. D. *J. Appl. Phys.* **2000**, *87*, 6007−6009.
(76) Chen, B.; Eddaoudi, M.; Reineke, T. M.; Kampf, J. W.; O'Keeffe, M.; Yaghi, O. M. *J. Am. Chem. Soc.* **2000**, *122*, 11559−11560.
(77) Lee, J.; Li, J.; Jagiello, J. *J. Solid State Chem.* **2005**, *178*, 2527−2532.
(78) In Table 3, we presented the NAO bond order for comparison with the CT and binding energy. In some molecules such as MeNC, MeCN, and CO, the bond order is parallel to the CT quantity but is not in N_2, C_2H_2, C_2H_2, N_2, and H_2.